Annals of the Academy of Romanian Scientists
Series on Physics and Chemistry
Online ISSN **2559 – 1061** Volume **11**, Number 1/**2026**

NUCLEAR EXCITATIONS WITH A MODIFIED SQUARE WELL COLLECTIVE POTENTIAL

R. Budaca[1,2],

Abstract

This study explores two γ-unstable solutions of the Bohr Hamiltonian for modified square well potentials: an infinite square well (ISW) with an adjustable step and a finite square well (FSW) with energy-dependent depth. The stepped ISW model is shown to be suitable for the description of shape coexistence and mixing phenomena in nuclei, as demonstrated through its application to the ^{200}Po nucleus. The analysis reveals various shape coexistence scenarios, with and without mixing, emerging at different energy states. On the other hand, the energy-dependent FSW model introduces a novel parameter-dependent eigensystem, preserving the algebraic structure of the energy-independent case, while generalizing the $E(5)$ critical dynamical symmetry. Applied to the ^{128}Xe nucleus, this model demonstrates improved agreement with experimental data compared to the $E(5)$ model.

keywords: Collective model, Energy levels, Transition probabilities

DOI: 10.56082/annalsarsciphyschem.2026.1.39

1 Introduction

The Schrödinger equation for a spherically symmetric square well potential of finite (FSW) or infinite (ISW) depth, is one of the cornerstone quantum problems. On one hand, it demonstrates the peculiarity of quantum mechanics, which allows a particle in the classically forbidden region. On another hand, it provides one of

[1]"Horia Hulubei" National Institute for R&D in Physics and Nuclear Engineering, Str. Reactorului 30, RO-077125, POB-MG6 Bucharest-Măgurele, Romania;
[2]Academy of Romanian Scientists, 3 Ilfov Street, Bucharest, 050044, sector 5, Romania;
E-mail: `rbudaca@theory.nipne.ro`
This work was supported by a grant of the Ministry of Research, Innovation and Digitization, CNCS - UEFISCDI, project number PN-IV-P1-PCE-2023-0273, within PNCDI IV

the few exactly solvable eigensystems, having the solutions determined in a fully algebraic manner. This aspect makes it an indispensable tool for modeling quantum effects, along with the quantum harmonic oscillator. For example, it has various applications in realistic physical systems, such as confined atoms [1], quantum dots [2, 3] or nuclear and quark systems [4, 5]. ISW and latter FSW were extremely useful in the early models for the short range nuclear interaction. FSW is the precursor of the well established Woods-Saxon mean-field [6].

One of the most notable and long lasting contribution of the square well problem to the understanding of nuclear phenomena is related to the concept of critical points for a shape phase transition. The introduction of the $E(5)$ [7] model for the transition between low and high deformation of a triaxially soft nuclear surface, opened a new field in nuclear structure studies. The $E(5)$ critical point is basically a solution of the five-dimensional Bohr Hamiltonian (BH) [8] for an ISW potential, in the axial deformation variable. The algebraic structure of the $E(5)$ exact solution ascribes a dynamical symmetry for the critical shape fluctuation model. It was found that the same symmetry properties can be reproduced within the Interacting Boson Model [9], providing thus a microscopic origin for the critical behavior. The same idea was replicated also for nuclear surfaces with a stable axial symmetry, giving rise to the $X(5)$ critical point model [10], with a more widespread experimental realization. Note however that $X(5)$ contains some approximations and is therefore just a partial dynamical symmetry [11].

By considering diverse collective conditions, other critical point models based on ISW followed: $X(3)$ for prolate γ-rigid nuclei [12], $Z(4)$ and $T(4)$ for triaxial γ-rigid shapes [13, 14], $Z(5)$ for triaxial γ-stable shapes [15]. Analytical generalizations on the shape phase space level provided the $X(4)$ model resulting from the equal mixing between γ-stable/unstable conditions [16, 17], and fractional versions of various critical point symmetries [18]. A natural extension of the $E(5)$ and $X(5)$ models is by means of coupling to single-particle degrees of freedom, for the description of odd mass nuclei [19, 20, 21, 22, 23]. The criticality of ISW solutions within a BH setting was also exploited in connection to triaxiality, for the construction of the $Y(5)$ model [24], or in relation to the octupole deformation [25, 26, 27, 28, 29]. Presently, the $E(5)$ and $X(5)$ solutions are employed with success as basis states for efficient diagonalization of double well collective potentials [30, 31, 32, 33, 34, 35, 36, 37]. It must be noted that FSW solutions for the BH were also forwarded, for the relaxation of the critical spectral signatures of the $E(5)$ [38] and $Z(5)$ [39] models. In the same context, the confined β-soft model [40] deserves a mention because it introduces an adjustable position of the inner potential wall.

In this study, one considers two recently proposed extensions of the BH with ISW and FSW potentials. Both models are described here within the γ-unstable conditions, and can be considered as generalizations of the $E(5)$ critical model. Nevertheless, it will be shown that the proposed models have much more to offer than the recovering of the $E(5)$ behavior in specific parameter limits. In one case, a finite step is introduced in the ISW potential [41]. The solution is analytically worked out in the next Section, as a function of the step's position and height. In the second case, one exploits the fact that the symmetry properties of exact solutions can be extended by considering the associated potentials with energy dependent coupling constants. This modification preserves the algebraic analytical structure of the original energy independent case [42, 43], but with a new parameter-dependence of the eigensystem. This formalism was applied in the past to various potentials in connection to BH [44, 45, 46, 47, 48]. Here it is presented in Sec. 3, for a FSW potential of an energy-dependent height [49]. The numerical implementation of the two models is addressed in Sec. 4, with a new experimental realization example for each. The conclusions will be summarized in the last Section.

2 Collective Hamiltonian for a γ-unstable nuclear surface

The quantum fluctuations of a nuclear surface with quadrupole deformation is described by two shape variables and three rotational angles. The former two are usually expressed by the deviation β from spherical shape, and the angular variable γ representing the deviation from axial symmetry. The β and γ shape variables are formally known as axial and respectively triaxial deformation. The five dimensional Bohr Hamiltonian [8] can then be written as

$$\hat{H}_{BM} = -\frac{\hbar^2}{2B}\left[\frac{1}{\beta^4}\frac{\partial}{\partial\beta}\beta^4\frac{\partial}{\partial\beta} + \frac{\hat{\Lambda}^2}{\beta^2}\right] + V(\beta,\gamma), \tag{2.1}$$

where $V(\beta,\gamma)$ is the potential function, while B is a mass parameter considered here as shape-independent. The operator

$$\hat{\Lambda}^2 = -\frac{1}{\sin 3\gamma}\frac{\partial}{\partial\gamma}\sin 3\gamma\frac{\partial}{\partial\gamma} + \sum_{k=1}^{3}\frac{\hat{L}_k^2}{4\sin^2(\gamma - 2\pi k/3)}, \tag{2.2}$$

denotes the $SO(5)$ Casimir operator and describes the coupling of the triaxial deformation with the rotational degrees of freedom (the set Ω of three Euler angles) involved in the action of the intrinsic angular momentum operators $\hat{L}_k$. The eigenvalue problem of the above operator is well known [50]

$$\hat{\Lambda}^2\mathcal{Y}_{\tau\alpha LM}(\gamma,\Omega) = \tau(\tau+3)\mathcal{Y}_{\tau\alpha LM}(\gamma,\Omega), \tag{2.3}$$

with a $SO(5)$ spherical harmonics $\mathcal{Y}_{\tau\alpha LM}(\gamma,\Omega)$ [51] as an eigenfunction and an eigenvalue defined in terms of the seniority quantum number τ [52]. Besides the seniority, the $SO(5)$ spherical harmonics are also indexed by the intrinsic angular momentum L, its projection M in the laboratory frame of reference, as well as an additional order α distinguishing multiple occurrences of the same angular momentum within a state of certain seniority.

If the potential depends only on the axial deformation, $V(\beta,\gamma) = V(\beta)$, the Hamiltonian (2.1) will contain the $SO(5)$ symmetry. This specific instance of the Bohr Hamiltonian is referred to as γ-unstable, due to the maximal spread of the wave function probability distribution in the triaxial deformation γ. The resulted symmetry properties of the γ-unstable case allows an exact separation of variables by means of a factorized wave function:

$$\Psi_{\xi\tau\alpha LM} = f(\beta)\mathcal{Y}_{\tau\alpha LM}(\gamma,\Omega). \tag{2.4}$$

which, after integration over the $SO(5)$ degrees of freedom, leads to the following β equation:

$$\left[-\frac{1}{\beta^4}\frac{\partial}{\partial\beta}\beta^4\frac{\partial}{\partial\beta} + \frac{\tau(\tau+3)}{\beta^2} + v(\beta)\right] f(\beta) = \varepsilon f(\beta), \tag{2.5}$$

where one introduced the reduced potential $v(\beta) = 2BV(\beta)/\hbar^2$ and the reduced energy $\varepsilon = 2BE/\hbar^2$. By the change of function $\tilde{f}(\beta) = f(\beta)/\beta^2$ one can extract an effective potential:

$$v^{\tau}_{eff}(\beta) = \frac{(\tau+1)(\tau+2)}{\beta^2} + v(\beta), \tag{2.6}$$

associated to a kinetic energy given just by a second order derivative. The fact that this effective potential is state dependent and contains the centrifugal interaction is useful for a one-to-one correlation with the total wave function. In what follows, one will present the solution of Eq. (2.5) with two options for the external potential $v(\beta)$. Before doing this, it is instructive to give the general expression for the transition probability in the case of γ-unstable conditions. The most relevant observable in this sense is the $E2$ transition. Its reduced probability rate is calculated as follows [45, 53, 54, 55]:

$$\begin{aligned} B(E2; L\tau n \rightarrow L'\tau' n') &= t_2(\tau'\alpha' L'; 112||\tau\alpha L)^2 \left(B_{\tau n;\tau' n'}\right)^2 \\ &\quad\times \left(\sqrt{\frac{\tau}{2\tau+3}}\delta_{\tau,\tau'+1} + \sqrt{\frac{\tau+3}{2\tau+3}}\delta_{\tau,\tau'-1}\right)^2, \end{aligned} \tag{2.7}$$

where the states are indexed by the angular momentum L, seniority τ and the so called β quantum number indexing the solutions of Eq. (2.5). The β matrix element

$$B_{\tau n;\tau' n'} = \langle f_{\tau n}(\beta)|\beta|f_{\tau' n'}(\beta)\rangle, \tag{2.8}$$

is calculated with a specific metric to each considered model, while t_2 is a scaling factor and $(\tau'\alpha' L'; 112||\tau\alpha L)$ is the $SO(5)$ Clebsch-Gordan coefficient [51].

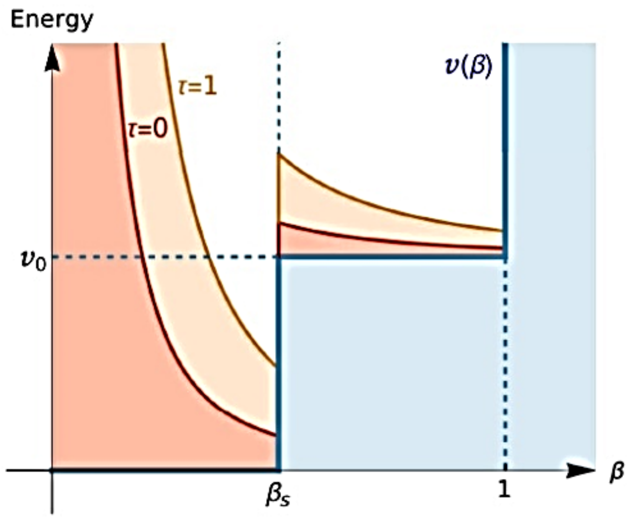

Figure 1: Reduced stepped potential $v(\beta)$ (3.1) and its effective instances $v^{\tau}_{eff}(\beta)$ defined by Eq.(2.6) when $\tau = 1, 2$ for $v_0 = 50$ and $\beta_s = 0.5$.

3 Infinite square well potential with an adjustable step

Here we consider an ISW potential with a step:

$$v(\beta) = \begin{cases} 0, & \beta \leq \beta_s, \\ v_0, & \beta_s < \beta \leq 1, \\ \infty, & \beta > 1. \end{cases} \tag{3.1}$$

$\beta_s \in [0, 1]$ denotes the position of the step and $v_0 > 0$ represents its height. The shape of this potential is shown in Fig. 1, along with few instances for its corresponding effective version (2.6). As can be seen, the conjunction of the step with a centrifugal contribution, leads to a two-pocket shape of the effective potential which is especially suited for shape coexistence and mixing phenomena [41].

The solutions of Hamiltonian (2.1) for this potential, were worked out in Ref. [41]. Basically, for $\beta < \beta_s$ the solution is given up to a factor, by a Bessel function of the first kind J_ν [56]:

$$f_{<\beta_s}(\beta) = A\beta^{-3/2} J_\nu(k_{<\beta_s}\beta), \;\; k_{<\beta_s} = \sqrt{\varepsilon}, \tag{3.2}$$

where A is a normalization constant and $\nu = \tau + 3/2$. When $\beta > \beta_s$, one has two types of solutions:

$$f^{\gtrless}_{>\beta_s}(\beta) = A\beta^{-3/2} J_\nu(k_{<\beta_s}\beta_s) \frac{Y_\nu(k^{\gtrless}_{>\beta_s}) J_\nu(k^{\gtrless}_{>\beta_s}\beta) - J_\nu(k^{\gtrless}_{>\beta_s}) Y_\nu(k^{\gtrless}_{>\beta_s}\beta)}{J_\nu(k^{\gtrless}_{>\beta_s}\beta_s) Y_\nu(k^{\gtrless}_{>\beta_s}) - J_\nu(k^{\gtrless}_{>\beta_s}) Y_\nu(k^{\gtrless}_{>\beta_s}\beta_s)}, \tag{3.3}$$

$$k^{\gtrless}_{>\beta_s} = \sqrt{\varepsilon - v_0}, \tag{3.4}$$

for $\varepsilon > v_0$, and

$$f^{<}_{>\beta_s}(\beta) = A\beta^{-3/2}J_\nu(k_{<\beta_s}\beta_s)\frac{K_\nu(k^{<}_{>\beta_s})I_\nu(k^{<}_{>\beta_s}\beta) - I_\nu(k^{<}_{>\beta_s})K_\nu(k^{<}_{>\beta_s}\beta)}{I_\nu(k^{<}_{>\beta_s}\beta_s)K_\nu(k^{<}_{>\beta_s}) - I_\nu(k^{<}_{>\beta_s})K_\nu(k^{<}_{>\beta_s}\beta_s)}, \quad (3.5)$$

$$k^{<}_{>\beta_s} = \sqrt{v_0 - \varepsilon}, \quad (3.6)$$

for $\varepsilon < v_0$. Y_ν is the Bessel function of the second kind, whereas I_ν and K_ν are modified Bessel functions of the first and respectively the second kind [56].

Finally, the total β wave function can be expressed in a compact way as:

$$f^{step}_{\tau n}(\beta) = f_{<\beta_s}(\beta)u_{\beta_s}(\beta) + f^{\lessgtr}_{>\beta_s}(\beta)[1 - u_{\beta_s}(\beta)]u_1(\beta), \quad (3.7)$$

where $n = 0, 1, ...$ is a β quantum number and with

$$u_{\beta_s}(\beta) = \begin{cases} 0, \beta < \beta_s \\ 1, \beta \geq \beta_s, \end{cases} \quad (3.8)$$

denoting the unit step function [57]. The remaining factor A is fixed by imposing the normalization to unity of the total wave function:

$$\int_0^{\beta_s} |f_{<\beta_s}|^2 \beta^4 d\beta + \int_{\beta_s}^1 \left|f^{\lessgtr}_{>\beta_s}\right|^2 \beta^4 d\beta = 1. \quad (3.9)$$

The same piece-wise integration scheme is used for the computation of the $B_{\tau n;\tau' n'}$ transition matrix elements.

The combined continuity condition at β_s:

$$\left.\frac{1}{f_{<\beta_s}(\beta)}\frac{df_{<\beta_s}(\beta)}{d\beta}\right|_{\beta_s} = \left.\frac{1}{f^{\lessgtr}_{>\beta_s}(\beta)}\frac{df^{\lessgtr}_{>\beta_s}(\beta)}{d\beta}\right|_{\beta_s}, \quad (3.10)$$

offers the spectral equation for the energy ε above/below v_0, which completes the description of the eigensystem.

4 Finite square well potential of an energy-dependent depth

Some quantum mechanical hypotheses must be reconsidered when dealing with energy dependent potentials [58, 59, 60, 61, 62]. For the purpose of present study, one can mention the following important aspects:

- The completeness condition is exactly satisfied only for the linear energy dependence. Therefore, one considers in this case a potential of the form

$$v(\beta, \varepsilon) = v_0(1 + a\varepsilon)u_1(\beta), \quad (4.1)$$

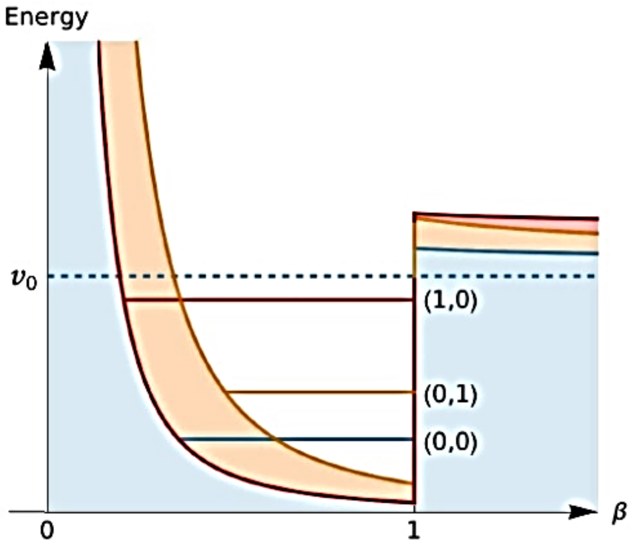

Figure 2: Reduced effective potential (2.6) with $v(\beta)$ given by Eq. (4.1) for the $(n, \tau) = (0, 0)$ (blue), $(1, 0)$ (red), and $(0, 1)$ (orange), when $v_0 = 50$ and $a = 0.005$.

where a is an adjustable slope parameter. The state evolution of the effective version for the above potential is depicted in Fig. 2. As can be seen, the energy dependence induces a distinct state evolution of the effective potential inside and outside the well.

- The scalar product and respectively the density probability distribution must be redefined to account for the energy dependence:

$$\rho(\beta) = |f(\beta)|^2 \beta^4 \left[1 - \frac{\partial v(\beta,\varepsilon)}{\partial \varepsilon}\right] = |f(\beta)|^2 \beta^4 \left[1 - a v_0 u_1(\beta)\right], \tag{4.2}$$

where f is the solution of Eq. (2.5) for the energy dependent potential (4.1). In order for the above quantity to serve as an acceptable probability density, one must have $a v_0 < 1$. Therefore, one has an upper limit $a < 1/v_0$ for the slope parameter.

The solutions are generally determined as in the usual case without energy dependence [63], with few particularities [49]. One distinguishes here two physical regions. Inside the well, the β wave function is defined as

$$f^{<}(\beta) = A' \beta^{-3/2} J_\nu(\kappa\beta), \ \kappa = \sqrt{\varepsilon}, \ \beta < 1. \tag{4.3}$$

The wave function outside of the well is respectively given by

$$f^{>}(\beta)=A'\beta^{-3/2}\frac{J_\nu(\kappa)H_\nu^{(1)}(i\lambda\beta)}{H_\nu^{(1)}(i\lambda)\sqrt{1-av_0}},\ \lambda=\sqrt{v_0(1+a\varepsilon)-\varepsilon},\ \beta>1. \tag{4.4}$$

where A' is a normalization constant, $H_\nu^{(1)}$ is the Hankel function of the first kind [56], and $\nu=\tau+3/2$.

Once again, the combined continuity condition at $\beta=1$:

$$\left.\frac{1}{f^{<}(\beta)}\frac{df^{<}(\beta)}{d\beta}\right|_{\beta=1}=\left.\frac{1}{f^{>}(\beta)}\frac{df^{>}(\beta)}{d\beta}\right|_{\beta=1}, \tag{4.5}$$

gives the energy ε in terms of seniority τ and the β quantum number $n=0,1,...$

The fragmented evolution of the normalization condition

$$\begin{aligned}&\int_0^1\left[f^{<}(\beta)\right]^2\beta^4d\beta+(1-av_0)\int_1^\infty\left[f^{>}(\beta)\right]^2\beta^4d\beta= \\ &(A')^2\left\{\int_0^1\left[J_\nu(\kappa\beta)\right]^2\beta d\beta+\left[\frac{J_\nu(\kappa)}{H_\nu^{(1)}(i\lambda)}\right]^2\int_1^\infty\left[H_\nu^{(1)}(i\lambda\beta)\right]^2\beta d\beta\right\}=1,\end{aligned} \tag{4.6}$$

determines the factor A'. As the original state-independent case, the present model has a finite number of bound states. If a certain state reaches the well's edge, one has $\varepsilon=v_0(1+a\varepsilon)$. This condition provides a critical lower limit for the slope parameter a, as a function of the well depth v_0, which assures a certain number of bound states. It is worth noting that in the $a\rightarrow 1/v_0$ limit, when $\lambda\rightarrow\sqrt{v_0}$, the model has in principle an infinite number of bound states. This aspect begs a comparison with infinite square well model, which was realized in Ref. [49].

5 Numerical applications

Both eigenvalue problems presented above, reduce to a transcendental equation for the energy ε. These are solved here numerically, for a selected set of seniority quantum numbers, in a grid of parameter values with specific intervals identified from the graphical method. The gathered data is then used to obtain a description of the low lying spectra in even-even nuclei. This is done by fits to experimental energies normalized to the first excitation energy. The model is used only for the description of ground and β band states characterized by $L=2\tau$. The parameters deduced from energy levels are then used for predictions on electromagnetic transitions. This is realized by fixing the scale t_2 from Eq. (2.7), such that to reproduce the experimental $B(E2,2_g^+\rightarrow 0_g^+)$ value. The search for experimental realizations of the two models is guided by their structure. Thus, as was mentioned previously, the stepped ISW model is suitable for nuclei with shape coexistence phenomena. As a matter of fact,

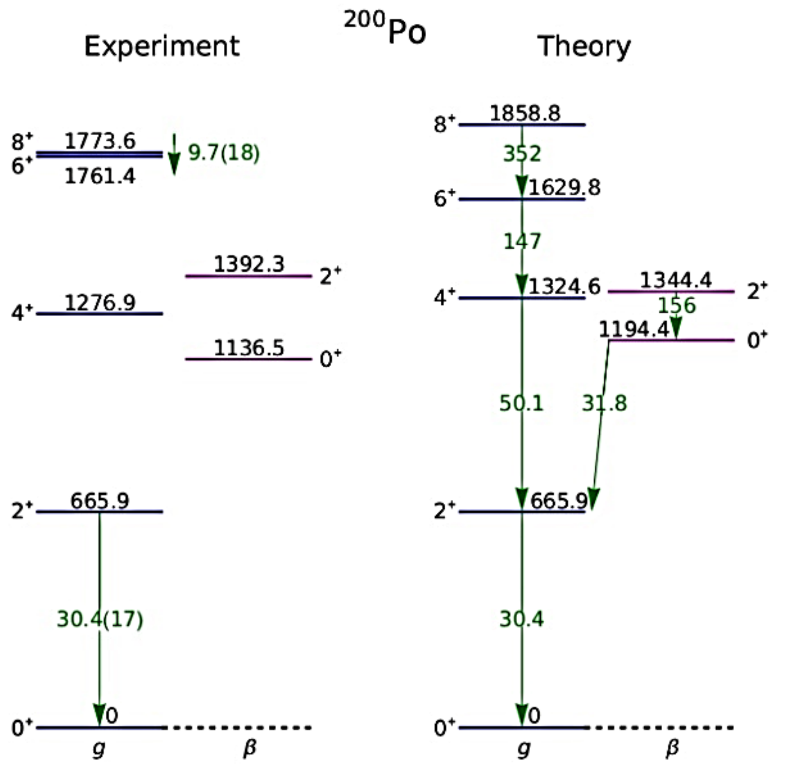

Figure 3: Experimental [64] and theoretical ground (g) and β band energy levels for the ^{200}Po nucleus. Energies are indexed by total angular momentum $L = 2\tau$ and given in keV, while transition probabilities are expressed in W.u. values.

its proof of concept application was on a series of Te nuclei [41], known for shape coexistence implications coming from intruder configurations. This mechanism is specific to nuclei with few nucleons above or below closed shells. Following this pattern, one selected the ^{200}Po nucleus as an experimental example of the stepped ISW γ-unstable model. From Fig. 3, one can see a very good agreement with experimental energy levels, given its peculiar dynamical evolution.

The specific pattern of the ^{200}Po energy spectrum can be better understood from Fig. 4, where one matched the corresponding effective potential with its wave function. One can thus conclude from the relative position of the states and their corresponding effective potential barrier, that ground band states with $\tau = 0, 1$ ($L = 0, 2$), are completely localized in the region before the step, with a smaller deformation. Whereas the next excited states are spread over both potential regions. This is exactly confirmed by the density of deformation probability distribution, which shows a transition from low to high deformation in the ground band at $\tau = 2$

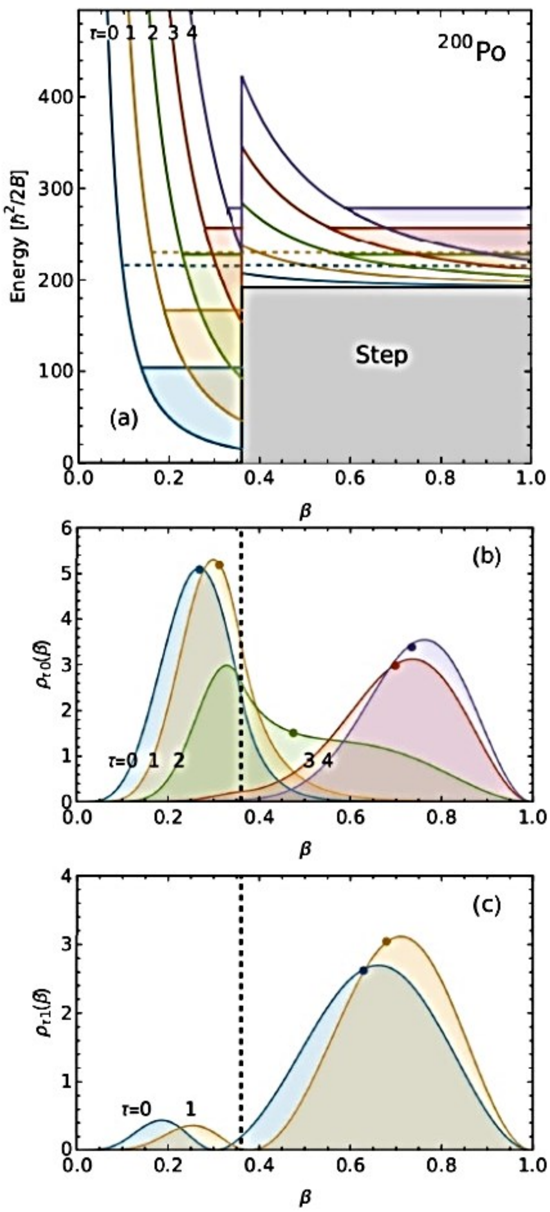

Figure 4: Theoretical effective potentials $v^{\tau}_{eff}(\beta)$ with a step of position $\beta_s = 0.36$ and height $v_0 = 192$ (a), and the probability distribution $\rho_{\tau n}(\beta) = [f^{step}_{\tau n}(\beta)]^2\beta^4$ for $\tau = 0, 1, 2, 3, 4$ ground band states (b) and β excited states with $\tau = 0, 1$ (c), plotted as a function of β for the ^{200}Po nucleus. Solid(dashed) lines are for $n = 0(n = 1)$ energy levels. Points on the density probability curves show the associated average deformation $\langle\beta\rangle_{\tau n}$.

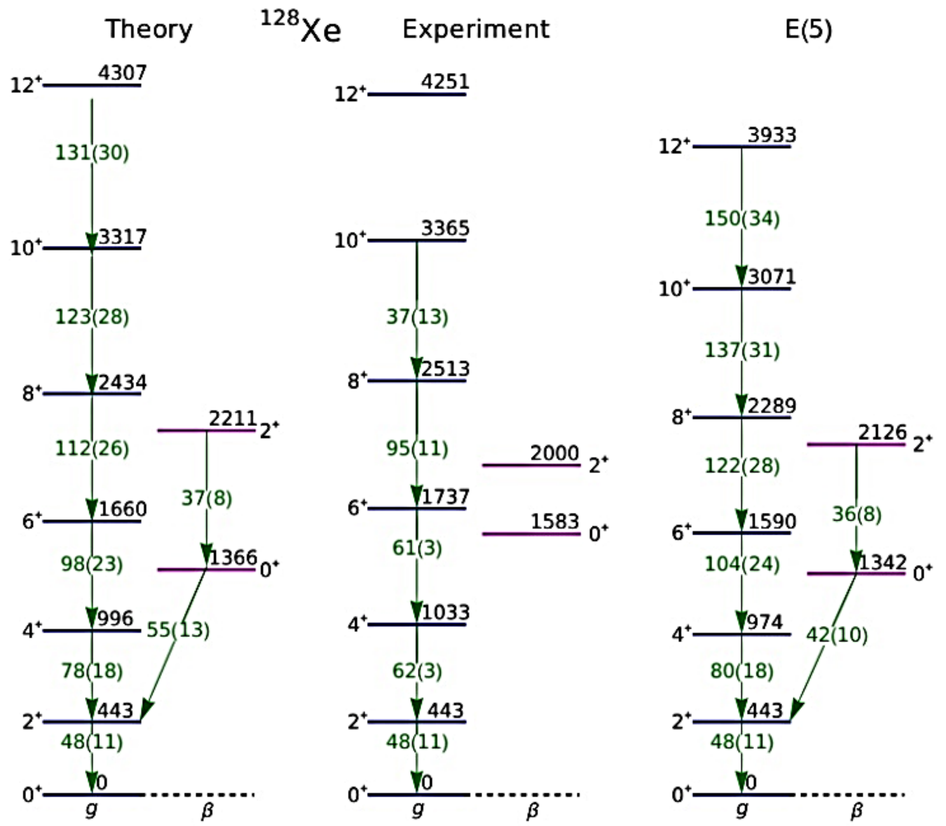

Figure 5: Comparison between the theoretical and experimental [66] energy spectra of the ^{128}Xe nucleus. The corresponding $E(5)$ spectrum [7] is also shown for reference. The states are indexed by the angular momentum $L = 2\tau$. The theoretical calculations are performed for an energy dependent depth, in the limit $a \to 1/v_0$ when $v_0 = 23$.

$(L = 4)$. As a matter of fact, the corresponding $\tau \geq 2$ $(L \geq 4)$ states exhibit a coexistence between the low and high deformation with a substantial amount of mixing, reflected in a reallocation of deformation probability besides the main peak of the associated wave function probability distribution. The ground band states with $\tau = 3, 4$ $(L = 6, 8)$ are then predominantly localized in the second potential pocket. This transition explains the contraction of the ground band energy spectrum. A study of the probability distribution in the β excited states, shows that although the one node vibrational behavior of these states is preserved, their high deformation turning point is substantially favored. This aspect demonstrates an another type of shape coexistence, that is without mixing. More precisely, the $\tau = 0, 1$ $(L = 0, 2)$

ground band states are of low deformation, while the same τ states from the β band can be considered as belonging to a separate high deformation configuration. The theoretical calculations for the transition probabilities in ^{200}Po, predict an overall increase with angular momentum. This trend is however not confirmed by the single experimental data available for the higher states.

In order to avoid premature band terminations, the energy-dependent FSW model is considered in its $a \rightarrow 1/v_0$ limit, which assures an unlimited number of bound states. This aspect obviously renders the proposed model as a generalization of the $E(5)$ critical dynamical symmetry [7]. As a matter of fact, considering the depth v_0 as the sole adjustable parameter, $E(5)$ properties can be recovered in the present model for very high values of v_0. As a demonstrative example of the usefulness for such a generalization, one applied the model to the $E(5)$ candidate nucleus ^{128}Xe [65]. Fig. 5 shows that the present model calculations improves the agreement with experiment in comparison to the $E(5)$ description. This is most obvious from the rotational pattern of the ground band, where the last two experimental states are collective continuations and not the yrast levels built on quasiparticle alignments. The position of the β band states are only approximately described by both theoretical models. Another distinction from the $E(5)$ spectral characteristics refers to the fact that in the present model the transition probabilities between ground band states are subsided, a fact which is in a better correlation with experiment. The visible differences between the present model and the $E(5)$ spectrum comes from the very small starting depth $v_0 = 23$.

6 Conclusions

The study explores two solutions of the γ-unstable Bohr Hamiltonian with modified square well potentials, specifically an infinite square well with an adjustable step and a finite square well with energy-dependent depth. The stepped ISW model is particularly suited for describing shape coexistence and mixing phenomena in nuclei, as demonstrated with the ^{200}Po nucleus. The analysis of the ^{200}Po nucleus reveals a transition from low to high deformation in the ground band at $L = 4$, with states exhibiting shape coexistence and mixing. The high deformation of the β excited states in comparison to the low deformation of the low lying ground band states, shows a different type of shape coexistence in the ^{200}Po nucleus. That is a shape coexistence without mixing, reflected in separate spectral structures of distinct deformation. The energy-dependent FSW model introduces a novel parameter-dependent eigensystem, which preserves the algebraic structure of the original energy-independent case. It generalizes the $E(5)$ critical dynamical symmetry, in the upper limit of the energy dependence slope, by means of an adjustable initial depth. As a result, the theoretical calculations for the ^{128}Xe nucleus show better alignment with experimental data compared to the $E(5)$ model. The fact that both models offer good agreement with experimental data, validates their ability to describe collective excitations within shape phase transitions. In conclusion, the present study highlights the potential of these models to provide deeper insights into nuclear structure and dynamics, particularly in cases involving shape coexistence and critical phenomena.

References

[1] J.-P. Connerade, V. K. Dolmatov, and S. T. Manson, J. Phys. B **32**, L395 (1999).

[2] B. Szafran, J. Adamowski, and B. Stébé, J. Phys.: Condens. Matter **10**, 7575 (1998).

[3] D. V. Melnikov and W. Beall Fowler, Phys. Rev. B **64**, 245320 (2001).

[4] R. Layeghnejad, M. Zare, and R. Moazzemi, Phys. Rev. D **84**, 125026 (2011).

[5] Bing-Nan Lu, En-Guang Zhao, and Shan-Gui Zhou, Phys. Rev. C **88**, 024323 (2013).

[6] R. D. Woods and D. S. Saxon, Phys. Rev. **95**, 577 (1954).

[7] F. Iachello, Phys. Rev. Lett. **85**, 3580 (2000).

[8] A. Bohr and B. R. Mottelson, *Nuclear Structure*, Vol. 2 (Benjamin, Reading, Massachusetts, 1975).

[9] F. Iachello and A. Arima, *The Interacting Boson Model*, (Cambridge University Press, Cambridge, 1987).

[10] F. Iachello, Phys. Rev. Lett. **87**, 052502 (2001).

[11] D. Bonatsos, E. A. McCutchan, and R. F. Casten, Phys. Rev. Lett. **101**, 022501 (2008).

[12] D. Bonatsos, D. Lenis, D. Petrellis, P. A. Terziev, and I. Yigitoglu, Phys. Lett. B **632**, 238 (2006).

[13] D. Bonatsos, D. Lenis, D. Petrellis, P. A. Terziev, and I. Yigitoglu, Phys. Lett. B **621**, 102 (2005).

[14] Y. Zhang, F. Pan, Y. X. Liu, Y. A. Luo, and J. P. Draayer, Phys. Rev. C **96**, 034323 (2017).

[15] D. Bonatsos, D. Lenis, D. Petrellis, and P. A. Terziev, Phys. Lett. B **588**, 172 (2004).

[16] R. Budaca and A. I. Budaca, Phys. Lett. B **759**, 349 (2016).

[17] R. Budaca and A. I. Budaca, Phys. Rev. C **94**, 054306 (2016).

[18] M. M. Hammad, Nucl. Phys. A **1011**, 122203 (2021).

[19] F. Iachello, Phys. Rev. Lett. **95**, 052503 (2005).

[20] C. E. Alonso, J. M. Arias, and A. Vitturi, Phys. Rev. Lett. **98**, 052501 (2007).

[21] Y. Zhang, F. Pan, Y. X. Liu, Z. F. Hou, and J. P. Draayer, Phys. Rev. C **82**, 034327 (2010).

[22] Y. Zhang, F. Pan, Y. X. Liu, Y. A. Luo, and J. P. Draayer, Phys. Rev. C **84**, 034306 (2011).

[23] Y. Zhang, F. Pan, Y. X. Liu, and J. P. Draayer, Phys. Rev. C **84**, 054319 (2011).

[24] F. Iachello, Phys. Rev. Lett. **91**, 132502 (2003).

[25] P. G. Bizzeti and A. M. Bizzeti-Sona, Phys. Rev. C **70**, 064319 (2004).

[26] D. Lenis and D. Bonatsos, Phys. Lett. B **633**, 474 (2006).

[27] R. Budaca, P. Buganu, and A. I. Budaca, Phys. Rev. C **106**, 014311 (2022).

[28] R. Budaca, A. I. Budaca, and P. Buganu, Phys. Scr. **99**, 035309 (2024).

[29] R. Budaca, EPL **151** 34002 (2025).

[30] R. Budaca, P. Buganu, and A. I. Budaca, Phys. Lett. B **776**, 26 (2018).

[31] R. Budaca and A. I. Budaca, EPL **123**, 42001 (2018).

[32] R. Budaca, A. I. Budaca, and P. Buganu, J. Phys. G: Nucl. Part. Phys. **46**, 125102 (2019).

[33] R. Budaca, P. Buganu, and A. I. Budaca, Nucl. Phys. A **990**, 137 (2019).

[34] A. Ait Ben Mennana, R. Benjedi, R. Budaca, P. Buganu, Y. EL Bassem, A. Lahbas, and M. Oulne, Phys. Scr. **96**, 125306 (2021).

[35] A. Ait Ben Mennana, R. Benjedi, R. Budaca, P. Buganu, Y. EL Bassem, A. Lahbas, and M. Oulne, Phys. Rev. **105**, 034347 (2022).

[36] R. Benjedi, R. Budaca, P. Buganu, Y. EL Bassem, A. Lahbas, and M. Oulne, Phys. Scr. **99**, 055307 (2024).

[37] P. Buganu and R. Budaca, Nucl. Phys. A **1067**, 123311 (2026).

[38] M. A. Caprio, Phys. Rev. C **65**, 031304(R) (2002).

[39] I. Inci, I. Boztosun, and Y. E. Gonen, J. Phys. G: Nucl. Part. Phys. **39**, 085112 (2012).

[40] N. Pietralla and O. M. Gorbachenko, Phys. Rev. C **70**, 011304(R) (2004).

[41] R. Budaca and A. I. Budaca, Eur. Phys. J. Plus **136**, 983 (2021).

[42] R. Yekken, M. Lassaut, and R. J. Lombard, Ann. Phys. (NY) **338**, 195 (2013).

[43] R. Budaca, Ann. Acad. Rom. Sci. Ser. Math. Appl. **9**, 205 (2017).

[44] R. Budaca, Phys. Lett. B **751**, 39 (2015).

[45] R. Budaca, Eur. Phys. J. A **52**, 314 (2016).

[46] A. I. Budaca and R. Budaca, Phys. Scr. **92**, 084001 (2017).

[47] A. I. Budaca and R. Budaca, Phys. Rev. C **101**, 064318 (2020).

[48] R. Budaca, Ann. Acad. Rom. Sci. Ser. Phys. Chem. Sci **5**, 7 (2020).

[49] R. Budaca, Eur. Phys. J. Plus **140**, 344 (2025).

[50] D. R. Bes, Nucl. Phys. **10**, 373 (1959).

[51] D. J. Rowe, P. S. Turner, and J. Repka, J. Math. Phys. **45**, 2761 (2004).

[52] G. Rakavy, Nucl. Phys. **4**, 289 (1957).

[53] R. Budaca, A. I. Budaca, and P. Buganu, J. Phys. G: Nucl. Part. Phys. **46**, 125102 (2019).

[54] D. J. Rowe, J. Phys. A: Math. Gen. **38**, 10181 (2005).

[55] D. J. Rowe and P. S. Turner, Nucl. Phys. A **753**, 94 (2005).

[56] F. Bowman, *Introduction to Bessel Functions*, (New York, Dover, 1958).

[57] M. Abramowitz and I. A. Stegun, *Handbook of Mathematical Functions with Formulas, Graphs, and Mathematical Tables*, 9th printing (New York: Dover, 1972).

[58] J. Formánek, R. J. Lombard, and J. Mareš, Czech. J. Phys. **54**, 289 (2004).

[59] G. P. Lepage, Phys. Rev. A **16**, 863 (1977).

[60] B. H. McKellar and C. M. McKay, Aust. J. Phys. **36**, 607 (1983).

[61] V. A. Rizov, H. Sazdjian, and I. T. Todorov, Ann. Phys. **165**, 59 (1985).

[62] H. Sazdjian, J. Math. Phys. **29**, 1620 (1988).

[63] B. H. Bransden and C. J. Joachain, *Quantum Mechanics*, 2nd edition (Prentice Hall, 2000).

[64] F. G. Kondev, Nucl. Data Sheets **192**, 1 (2023).

[65] R. M. Clark, M. Cromaz, M. A. Deleplanque, M. Descovich, R. M. Diamond, P. Fallon, I. Y. Lee, A. O. Macchiavelli, H. Mahmud, E. Rodriguez-Vieitez, F. S. Stephens, and D. Ward, Phys. Rev. C **69**, 064322 (2004).

[66] Z. Elekes and J. Timar, Nucl. data Sheets **129**, 191 (2015).